

---

# ERFACT: NON-MONOTONIC SMOOTH TRAINABLE ACTIVATION FUNCTIONS

---

A PREPRINT

Koushik Biswas

Sandeep Kumar

Shilpak Banerjee

Ashish Kumar Pandey

## ABSTRACT

An activation function is a crucial component of a neural network that introduces non-linearity in the network. The state-of-the-art performance of a neural network depends on the perfect choice of an activation function. We propose two novel non-monotonic smooth trainable activation functions, called ErfAct-1 and ErfAct-2. Experiments suggest that the proposed functions improve the network performance significantly compared to the widely used activations like ReLU, Swish, and Mish. Replacing ReLU by ErfAct-1 and ErfAct-2, we have 5.21% and 5.04% improvement for top-1 accuracy on PreactResNet-34 network in CIFAR100 dataset, 2.58% and 2.76% improvement for top-1 accuracy on PreactResNet-34 network in CIFAR10 dataset, 1.0%, and 1.0% improvement on mean average precision (mAP) on SSD300 model in Pascal VOC dataset.

**Keywords** Deep Learning · Trainable Activation Function

## 1 Introduction

The choice of activation function in a deep learning architecture can have a significant impact on the training and performance of the trained network. The machine learning community has so far relied on hand-designed activations like ReLU [1], Leaky ReLU [2] or their variants. ReLU, in particular, remains widely popular due to faster training times and decent performance. However, evidence suggests that considerable gains can be made when more sophisticated activation functions are used to design networks. For example, activation functions such as ELU [3], Parametric ReLU [4], ReLU6 [5], PAU [6], OPAU [7], ACON [8], Mish [9], GELU [10], Swish [11], TanhSoft [12], EIS [13], etc have appeared as powerful contenders to the traditional ones. Though ReLU remains a go-to choice in both research and practice, it has certain well-documented shortcomings such as non-zero mean [3], non-differentiability and negative missing, which leads to the infamous vanishing gradients problem (also known as the dying ReLU problem). Worth noting that prior to the introduction of ReLU, Tanh and Sigmoid were popularly used, but performance gains and training time gains achieved by ReLU led to their decline.

## 2 Related works and motivation

The newer activation functions are obtained by combining well-known functions with simple forms in various ways, often using hyper-parameters or trainable parameters. In the case of trainable parameters, we optimize them during the training process itself, yielding networks that are better fitted. In the case of trainable parameters, note that actual activation function curve may change in different layers during backpropagation. For example, SiLU [14] shows good performance over known activation functions while Swish [11] is a trainable version of SiLU, which is a non-linear, non-monotonic activation function. Among the activation mentioned in the previous section, Swish, PAU, TanhSoft, and OPAU are trainable activation functions. Swish and TanhSoft are non-monotonic activation functions, and both shows promise across a variety of deep learning tasks. Mish is one of the popular functions proposed recently and gained popularity due to its effectiveness in object detection task on COCO dataset [15] in Yolo [16] models. GELU is very similar to Swish and gained attention due to its effectiveness in computer vision and natural language processing tasks. It is also used in popular architectures like GPT-2 [17] and GPT-3 [18]. Apart from using a combination of known functions, a somewhat fundamentally different technique to construct activation functions is to use perturbation or approximations to well-known activation functions to remove some of the shortcomings yet retaining the positive

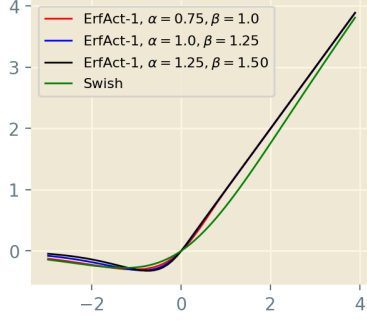


Figure 1: Swish and ErfAct-1 activation for different values of  $\alpha$  and  $\beta$

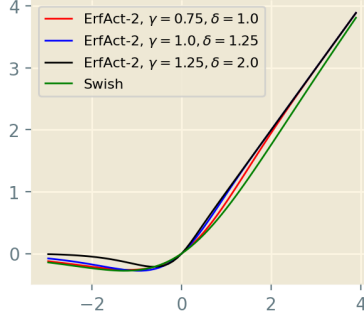


Figure 2: Swish and ErfAct-2 activation for different values of  $\gamma$  and  $\delta$

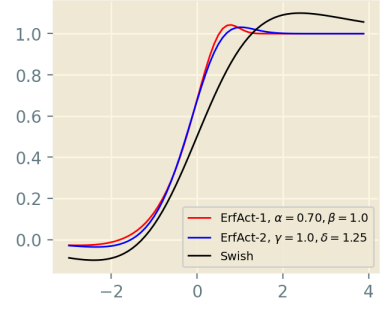


Figure 3: First order derivative of ErfAct-1, ErfAct-2, and Swish

aspects. Recent successful examples where this strategy was employed includes PAU and OPAU, which are activations based on approximation of Leaky ReLU by rational polynomials were constructed.

Motivated from these works, we have proposed two activation functions with trainable parameters, we call them ErfAct-1 and ErfAct-2 and shown that they are more effective than conventional activation functions like ReLU, Leaky ReLU, PReLU, ReLU6, Swish, Mish or GELU in a wide range of standard deep learning problems.

We summarize the paper as follows:

- We have proposed two new novel trainable activation functions, which are the smooth approximation of ReLU.
- In a wide range of deep learning tasks, the proposed functions outperform widely used activation functions.

### 3 ErfAct-1 and ErfAct-2

As motivated earlier, in this paper, we present, ErfAct-1 and ErfAct-2, two novel trainable activation functions which outperforms the widely used activations and has the potential to replace them. ErfAct-1 and ErfAct-2 is defined as

$$\text{ErfAct-1} : \mathcal{F}_1(x; \alpha, \beta) := x \operatorname{erf}(\alpha e^{\beta x}), \quad (1)$$

$$\text{ErfAct-2} : \mathcal{F}_2(x; \gamma, \delta) := x \operatorname{erf}(\gamma \ln(1 + e^{\delta x})) \quad (2)$$

where ‘erf’ is the error function also known as the Gauss error function and defined as

$$\operatorname{erf}(x) = \frac{2}{\sqrt{\pi}} \int_0^x e^{-t^2} dt \quad (3)$$

The corresponding derivatives of the proposed activations are

$$\frac{d}{dx} \mathcal{F}_1(x; \alpha, \beta) = \operatorname{erf}(\alpha e^{\beta x}) + \frac{2x\alpha\beta}{\sqrt{\pi}} e^{\beta x} e^{-(\alpha e^{\beta x})^2} \quad (4)$$

$$\frac{d}{dx} \mathcal{F}_2(x; \gamma, \delta) = \operatorname{erf}(\gamma \ln(1 + e^{\delta x})) + \frac{2x\gamma\delta}{\sqrt{\pi}} \frac{e^{\delta x}}{1 + e^{\delta x}} e^{-(\gamma \ln(1 + e^{\delta x}))^2} \quad (5)$$

where

$$\frac{d}{dx} \operatorname{erf}(x) = \frac{2}{\sqrt{\pi}} e^{-x^2} \quad (6)$$

ErfAct-1 and ErfAct-2 are non-monotonic, zero-centered, continuously differentiable, unbounded above but bounded below, and trainable functions. Figures 1 and 2 show the plots for  $\mathcal{F}_1(x; \alpha, \beta)$  and  $\mathcal{F}_2(x; \gamma, \delta)$  activation functions for different values of  $\alpha, \beta$ , and  $\gamma, \delta$  respectively. A comparison between the first derivative of  $\mathcal{F}_1(x; \alpha, \beta)$ ,  $\mathcal{F}_2(x; \gamma, \delta)$ ,

and Swish are given in Figures 3, different values of  $\alpha$ ,  $\beta$ , and  $\gamma$ ,  $\delta$  respectively. From the figures 1 and 2 it is evident that the parameters  $\alpha$ ,  $\beta$ , and  $\gamma$ ,  $\delta$  controls the slope of the curves for the proposed activations in both positive and negative axis. The proposed functions converges to some known functions for specific values of the parameters. For example,  $\mathcal{F}_1(x; 0, \beta)$ ,  $\mathcal{F}_2(x; 0, \delta)$  are zero function while  $\mathcal{F}_1(x; \alpha, 0)$ ,  $\mathcal{F}_2(x; \gamma, 0)$  are linear functions. The proposed functions can be seen as a smooth approximation of ReLU.

$$\lim_{\beta \rightarrow \infty} \mathcal{F}_1(x; \alpha, \beta) = \text{ReLU}(x),$$

$$\forall x \in \mathbb{R} \text{ for any fixed } \alpha > 0.$$

$$\lim_{\delta \rightarrow \infty} \mathcal{F}_2(x; \gamma, \delta) = \text{ReLU}(x),$$

$$\forall x \in \mathbb{R} \text{ for any fixed } \gamma > 0.$$

For any  $K$ , a compact (closed and bounded) subset of  $\mathbb{R}^n$ , the set of neural networks with ErfAct-1 (or ErfAct-2) activation functions is dense in  $C(K)$ , the space of all continuous functions over  $K$  (see [6]). This follows from the next proposition, as the proposed activation functions are not polynomials.

**Proposition (Theorem 1.1 in Kidger and Lyons, 2019 [19]) :-** Let  $\rho : \mathbb{R} \rightarrow \mathbb{R}$  be any continuous function. Let  $N_n^\rho$  represent the class of neural networks with activation function  $\rho$ , with  $n$  neurons in the input layer, one neuron in the output layer, and one hidden layer with an arbitrary number of neurons. Let  $K \subseteq \mathbb{R}^n$  be compact. Then  $N_n^\rho$  is dense in  $C(K)$  if and only if  $\rho$  is non-polynomial.

## 4 Experiments

We have compared our proposed activations against nine popular standard activation functions on different datasets and models on standard deep learning problems like image classification, object detection, semantic segmentation, and machine translation. The experimental results show that ErfAct-1 and ErfAct-2 outperform in most networks compared to the standard activations. For all our experiments, we have first initialized the parameters  $\alpha = 0.70$ ,  $\beta = 1.0$  for ErfAct-1 and  $\gamma = 1.0$ ,  $\delta = 1.25$  for ErfAct-2 and then updated via the backpropagation [20] algorithm (see [4]) according to (7) and for a single layer, the gradient of a hyper-parameter  $\rho$  is:

$$\frac{\partial L}{\partial \rho} = \sum_x \frac{\partial L}{\partial f(x)} \frac{\partial f(x)}{\partial \rho} \quad (7)$$

where  $L$  is the objective function,  $\rho \in \{\alpha, \beta, \gamma, \delta\}$  and  $f(x) \in \{\mathcal{F}_1(x; \alpha, \beta), \mathcal{F}_2(x; \gamma, \delta)\}$ . For all of our experiments, to make a fair comparison between all the activations, we have first trained a network with hyper-parameter settings with the ReLU activation function and then only replaced ReLU with the proposed functions and the baseline activations.

### 4.1 Image Classification

We present a detailed experimental comparison on MNIST [21], Fashion MNIST [22], CIFAR10 [23], CIFAR100 [23], and Tiny ImageNet [24] dataset for image classification problem. We have trained the datasets with different standard models and report the top-1 accuracy.

#### 4.1.1 MNIST, Fashion MNIST, and The Street View House Numbers (SVHN) Database

We first evaluate our proposed activation functions on the MNIST [21], Fashion MNIST [22], and SVHN [25] datasets with AlexNet [26] and VGG-16 [27] (with batch-normalization) models and results for 10-fold mean accuracy are reported in Table 1 and Table 2 respectively. More detailed experiments on these datasets on LeNet [28] and a custom-designed CNN architecture is reported in the appendix section. We don't use any data augmentation for MNIST or Fashion MNIST, while we use standard data augmentation like rotation, zoom, height shift, shearing for the SVHN dataset. From Table 1 and Table 2, it is clear that the proposed functions outperformed all the baseline activation functions in all the three datasets and the performance are stable clear from mean  $\pm$  standard deviation.

Activation Function	MNIST	Fashion MNIST	SVHN
ReLU	99.09±0.10	93.22±0.21	95.50±0.22
Swish	99.30±0.12	93.29±0.22	95.59±0.20
Leaky ReLU( $\alpha = 0.01$ )	99.15±0.13	93.30±0.22	95.50±0.28
ELU	99.29±0.13	93.20±0.25	95.60±0.20
Softplus	99.10±0.14	93.18±0.32	95.20±0.37
Mish	99.27±0.14	93.45±0.32	95.60±0.31
GELU	99.22±0.12	93.40±0.25	95.55±0.27
PReLU	99.15±0.16	93.37±0.31	95.42±0.39
ReLU6	99.11±0.10	93.26±0.26	95.47±0.24
ErfAct-1	<b>99.51±0.10</b>	<b>93.79±0.19</b>	<b>95.87±0.20</b>
ErfAct-2	<b>99.49±0.10</b>	<b>93.82±0.19</b>	<b>95.74±0.22</b>

Table 1: Comparison between different baseline activations and ErfAct-1 and ErfAct-2 activations on MNIST, Fashion MNIST, and SVHN datasets in AlexNet. 10-fold mean accuracy (in %) have been reported. mean±std is reported in the table.

Activation Function	MNIST	Fashion MNIST	SVHN
ReLU	99.05 ± 0.11	93.13 ± 0.23	95.09 ± 0.26
Swish	99.09 ± 0.09	93.34 ± 0.21	95.29 ± 0.20
Leaky ReLU( $\alpha = 0.01$ )	99.02 ± 0.14	93.17 ± 0.28	95.24 ± 0.23
ELU	99.01 ± 0.15	93.12 ± 0.30	95.15 ± 0.28
Softplus	98.97 ± 0.14	92.98 ± 0.34	94.94 ± 0.30
Mish	99.18±0.07	93.47±0.27	95.12 ±0.25
GELU	99.10±0.09	93.41±0.29	95.11 ±0.24
PReLU	99.01±0.09	93.12±0.27	95.14 ±0.24
ReLU6	99.20±0.08	93.25±0.27	95.22 ±0.20
ErfAct-1	<b>99.37±0.06</b>	<b>93.81±0.20</b>	<b>95.67±0.18</b>
ErfAct-2	<b>99.38±0.09</b>	<b>93.87±0.22</b>	<b>95.66±0.25</b>

Table 2: Comparison between different baseline activations, ErfAct-1, and ErfAct-2 activations on MNIST, Fashion MNIST, and SVHN datasets on VGG-16 network. We report results for 10-fold mean accuracy (in %). mean±std is reported in the table.

#### 4.1.2 CIFAR

Next we have considered more challenging datasets like CIFAR10 and CIFAR100 to compare the performance of baseline activations and ErfAct-1 and ErfAct-2. We have reported the Top-1 accuracy for both the datasets for mean of 12 different runs on Table 3 and Table 4 with VGG-16 (with batch-normalization) [27], PreActResNet-34 (PA-ResNet-34) [29], Densenet-121 (DN-121) [30], MobileNet V2 (MN V2) [31], Resnet-50 [32], Inception V3 [33], WideResNet 28-10 [34], and SqueezeNet [35] models. A more detailed experiments on these datasets with EfficientNet B0 (EN-B0) [36], LeNet [28], AlexNet (AN) [26], PreActResnet-18 [29], Deep Layer Aggregation (DLA) [37], Googlenet [38], Resnext [39], Xception [40], ShuffleNet [41], ResNet18 [32], and Network in Network [42] is reported in the appendix section. From all the tables it is evident that the training is stable (mean±std) and the proposed activations archive 1%-5% higher top-1 accuracy in most of models compared to the baselines. The networks are trained upto 100 epochs with Adam optimizer [43] with 0.001 learning rate, and 128 batch size. We have considered standard data augmentation methods like width shift, height shift, horizontal flip, rotation for both the datasets. The Figures 4 and 5 shows the learning curves on CIFAR100 dataset with PreActResNet-18 model for the baseline and the proposed activation functions and it is noticeable that training & test accuracy curve is higher and loss curve is lower respectively for ErfAct-1 and ErfAct-2 compared to the baseline activations.

#### 4.1.3 Tiny Imagenet

We consider a more challenging and important classification dataset Tiny Imagenet [24] which is a similar type of dataset like ILSVRC and consisting of 200 classes with RGB images of size  $64 \times 64$  with total 1,00,000 training images,

Activation Function	VGG-16	WRN 28-10	ResNet-50	PA-ResNet-34	DN-121	IN-V3	MN-V2	SQ-Net
ReLU	89.64 ±0.20	91.64 ±0.25	90.42 ±0.29	90.72 ±0.30	91.42 ±0.25	91.52 ±0.29	91.02 ±0.32	88.59 ±0.36
Leaky ReLU ( $\alpha = 0.01$ )	89.79 ±0.22	91.80 ±0.24	90.40 ±0.29	90.64 ±0.32	91.52 ±0.30	91.72 ±0.33	90.89 ±0.27	88.72 ±0.39
ELU	89.01 ±0.20	91.22 ±0.24	90.60 ±0.30	90.64 ±.30	91.44 ±0.34	91.45 ±0.39	91.23 ±0.30	88.52 ±0.30
Swish	90.24 ±0.18	92.21 ±0.20	90.91 ±0.22	91.99 ±0.24	92.22 ±0.23	92.42 ±0.27	91.89 ±0.26	89.23 ±0.32
Softplus	89.17 ±0.27	91.10 ±0.27	89.77 ±0.30	90.24 ±0.39	91.13 ±0.34	91.20 ±0.36	90.72 ±0.30	88.53 ±0.36
Mish	90.29 ±0.29	92.41 ±0.22	91.04 ±0.27	92.22 ±0.25	92.53 ±0.29	92.72 ±0.21	92.12 ±0.26	89.41 ±0.31
GELU	90.12 ±0.22	92.12 ±0.27	91.11 ±0.24	91.89 ±0.25	92.12 ±0.30	91.56 ±0.27	92.00 ±0.26	89.02 ±0.32
PReLU	89.64 ±0.20	91.10 ±0.29	90.64 ±0.29	90.60 ±0.32	90.85 ±0.33	90.69 ±0.37	91.02 ±0.36	88.25 ±0.38
ReLU6	89.82 ±0.25	91.54 ±0.20	90.89 ±0.24	90.65 ±0.22	90.72 ±0.26	90.87 ±0.29	90.62 ±0.28	88.48 ±0.36
ErfAct-1	<b>91.12</b> ±0.18	<b>93.21</b> ±0.19	<b>92.02</b> ±0.21	<b>93.30</b> ±0.20	<b>93.47</b> ±0.24	<b>93.52</b> ±0.26	<b>92.92</b> ±0.26	<b>90.12</b> ±0.28
ErfAct-2	<b>90.99</b> ±0.20	<b>93.51</b> ±0.20	<b>91.87</b> ±0.20	<b>93.48</b> ±0.18	<b>93.57</b> ±0.25	<b>93.21</b> ±0.30	<b>92.77</b> ±0.23	<b>90.42</b> ±0.29

Table 3: Comparison between different baseline activations and ErfAct-1 and ErfAct-2 on CIFAR10 dataset. Top-1 accuracy(in %) for mean of 12 different runs have been reported. mean±std is reported in the table.

Activation Function	VGG-16	WRN 28-10	ResNet-50	PA-ResNet-34	DN-121	IN-V3	MN-V2	SQ-Net
ReLU	61.12 ±0.55	69.40 ±0.39	62.20 ±0.45	60.59 ±0.52	69.64 ±0.34	68.40 ±0.42	68.49 ±0.39	64.53 ±0.46
Leaky ReLU ( $\alpha = 0.01$ )	61.29 ±0.59	69.29 ±0.32	62.12 ±0.39	60.72 ±0.54	69.85 ±0.32	68.29 ±0.49	68.22 ±0.34	64.77 ±0.51
ELU	61.58 ±0.54	69.12 ±0.39	62.53 ±0.45	60.10 ±.51	69.80 ±0.32	68.72 ±0.55	68.12 ±0.39	65.10 ±0.50
Swish	63.12 ±0.43	70.15 ±0.35	63.54 ±0.40	62.99 ±0.52	70.01 ±0.33	69.86 ±0.27	69.10 ±0.36	65.12 ±0.42
Softplus	60.13 ±0.57	68.12 ±0.49	62.32 ±0.49	59.55 ±0.57	69.10 ±0.54	68.17 ±0.49	67.72 ±0.39	64.85 ±0.56
Mish	63.71 ±0.45	70.45 ±0.32	63.42 ±0.42	63.22 ±0.50	70.54 ±0.30	70.10 ±0.31	69.55 ±0.40	65.59 ±0.48
GELU	63.42 ±0.50	69.58 ±0.35	63.52 ±0.48	63.17 ±0.59	70.18 ±0.30	70.01 ±0.39	69.61 ±.39	64.89 ±0.51
PReLU	60.89 ±0.54	69.42 ±0.45	62.29 ±0.47	60.87 ±0.50	69.81 ±0.39	68.20 ±0.51	68.67 ±0.45	64.55 ±0.52
ReLU6	61.52 ±0.51	69.99 ±0.40	62.56 ±0.48	69.86 ±0.50	70.13 ±0.37	68.80 ±0.36	68.49 ±0.36	64.86 ±0.49
ErfAct-1	<b>64.42</b> ±0.41	<b>71.42</b> ±0.30	<b>65.10</b> ±0.41	<b>65.80</b> ±0.50	<b>71.89</b> ±0.32	<b>71.51</b> ±0.35	<b>70.65</b> ±0.35	<b>66.12</b> ±0.40
ErfAct-2	<b>64.12</b> ±0.40	<b>71.49</b> ±0.37	<b>65.15</b> ±0.49	<b>65.63</b> ±0.45	<b>71.56</b> ±0.32	<b>71.31</b> ±0.30	<b>70.89</b> ±0.31	<b>65.92</b> ±0.42

Table 4: Comparison between different baseline activations and ErfAct-1 and ErfAct-2 on CIFAR100 dataset. Top-1 accuracy(in %) for mean of 12 different runs have been reported. mean±std is reported in the table.

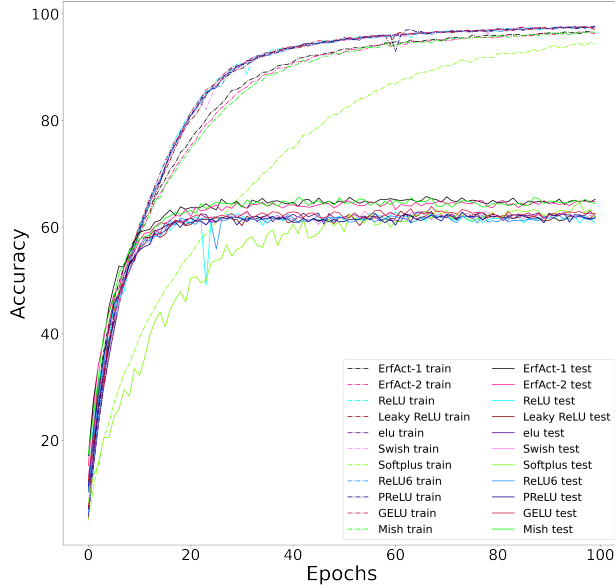


Figure 4: Top-1 Train and Test accuracy (higher is better) on CIFAR100 dataset with PreActResNet-18 network for different baseline activations, ErfAct-1, and ErfAct-2.

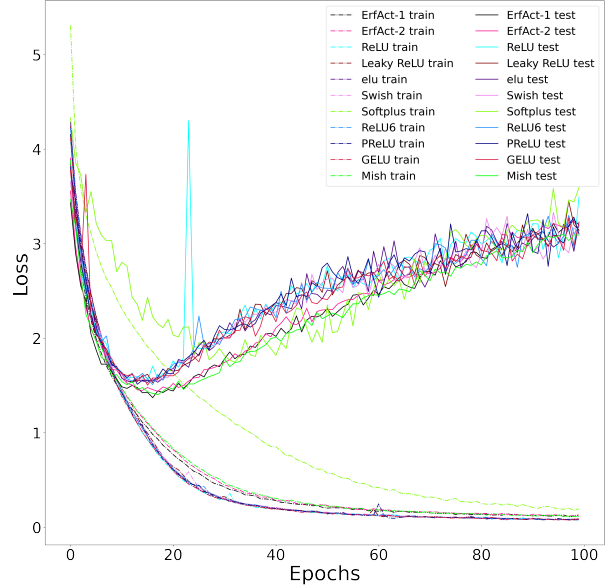


Figure 5: Top-1 Train and Test loss (lower is better) on CIFAR100 dataset with PreActResNet-18 network for different baseline activations, ErfAct-1, and ErfAct-2.

10,000 validation images, and 10,000 test images. To compare the performance, we have considered WideResNet 28-10 (WRN 28-10) [34] model and Top-1 accuracy is reported in table 5 for mean of 5 different runs. The model is trained with a batch size of 32, He Normal initializer [4], 0.2 dropout rate [44], adam optimizer [43], with initial learning rate(lr rate) 0.01, and lr rate is reduced by a factor of 10 after every 60 epochs up-to 300 epochs. We have considered the standard data augmentation methods like rotation, width shift, height shift, shearing, zoom, horizontal flip, fill mode. From the table, it is clear that the performance for the proposed functions are better than the baseline functions and stable (mean $\pm$ std) and got a boost in top-1 accuracy by 2.59% and 2.40% for ErfAct-1 and ErfAct-2 compared to ReLU.

Activation Function	Wide ResNet 28-10 Model
ReLU	61.61 $\pm$ 0.47
Swish	62.44 $\pm$ 0.49
Leaky ReLU( $\alpha = 0.01$ )	61.47 $\pm$ 0.44
ELU	61.99 $\pm$ 0.57
Softplus	60.42 $\pm$ 0.61
Mish	63.02 $\pm$ 0.57
GELU	62.64 $\pm$ 0.62
PReLU	61.25 $\pm$ 0.51
ReLU6	61.72 $\pm$ 0.56
ErfAct-1	<b>64.20<math>\pm</math>0.51</b>
ErfAct-2	<b>64.01<math>\pm</math>0.49</b>

Table 5: Comparison between different baseline activations and ErfAct-1 and ErfAct-2 on Tiny ImageNet dataset. Mean of 5 different runs for top-1 accuracy(in %) have been reported. mean $\pm$ std is reported in the table.

Activation Function	mAP
ReLU	77.2 $\pm$ 0.14
Swish	77.3 $\pm$ 0.11
Leaky ReLU( $\alpha = 0.01$ )	77.2 $\pm$ 0.19
ELU	75.1 $\pm$ 0.22
Softplus	74.2 $\pm$ 0.25
Mish	77.5 $\pm$ 0.14
GELU	77.3 $\pm$ 0.12
PReLU	77.2 $\pm$ 0.20
ReLU6	77.1 $\pm$ 0.15
ErfAct-1	<b>78.2<math>\pm</math>0.12</b>
ErfAct-2	<b>78.2<math>\pm</math>0.14</b>

Table 6: Comparison between different baseline activations and ErfAct-1 and ErfAct-2 on Object Detection problem on SSD 300 model in Pascal-VOC dataset. mean $\pm$ std is reported in the table.

## 4.2 Object Detection

Object detection is a standard problem in computer vision. In this section, we have reported our experimental results on challenging Pascal VOC dataset [45] with Single Shot MultiBox Detector(SSD) 300 [46] with VGG-16(with batch-normalization) [27] as the backbone network. The mean average precision (mAP) is reported in Table 6 for a mean of 5 different runs. The model is trained with batch size of 8, 0.001 learning rate, SGD optimizer [47, 48] with 0.9 momentum,  $5e^{-4}$  weight decay for 120000 iterations. The result are stable on different runs (mean $\pm$ std). We got around 1% boost in mAP for both ErfAct-1 and ErfAct-2 compared to ReLU.

## 4.3 Semantic Segmentation

Semantic segmentation is an important problem in deep learning. In this section, we present experimental results on the Cityscapes dataset [49]. We report the pixel accuracy and more on the U-net model[50]. The model is trained up to 250 epochs, with adam optimizer [43], learning rate  $5e^{-3}$ , batch size 32 and Xavier Uniform initializer [51]. A mean of 5 different runs on the test dataset is reported in table 7. We got around 1.97% and 1.89% boost on mIOU for ErfAct-1 and ErfAct-2 compared to ReLU.

## 4.4 Machine Translation

Machine Translation is a procedure in which text or speech is translated from one language to another language without the help of any human being. We consider the standard WMT 2014 English $\rightarrow$ German dataset for our experiment. The database contains 4.5 million training sentences. We train an attention-based 8-head transformer network [52] with Adam optimizer [43], 0.1 dropout rate [44], and train up to 100000 steps. We try to keep other hyperparameters similar as mentioned in the original paper [52]. We evaluate the network performance on the newstest2014 dataset using the BLEU score metric. The mean of 5 different runs is being reported on Table 8 on the test dataset(newstest2014). From the table, it is clear that the results are stable on different runs (mean $\pm$ std), and we got around 0.6% and 0.5% boost in BLEU score for ErfAct-1 and ErfAct-2 compared to ReLU.

Activation Function	Pixel Accuracy	mIOU
ReLU	79.60 $\pm$ 0.45	69.32 $\pm$ 0.30
Swish	79.71 $\pm$ 0.49	69.68 $\pm$ 0.31
Leaky ReLU ( $\alpha = 0.01$ )	79.41 $\pm$ 0.42	69.48 $\pm$ 0.39
ELU	79.27 $\pm$ 0.54	68.12 $\pm$ 0.41
Softplus	78.69 $\pm$ 0.49	68.12 $\pm$ 0.55
Mish	80.12 $\pm$ 0.45	69.87 $\pm$ 0.29
GELU	79.60 $\pm$ 0.39	69.51 $\pm$ 0.39
PReLU	78.99 $\pm$ 0.42	68.82 $\pm$ 0.41
ReLU6	79.59 $\pm$ 0.41	69.66 $\pm$ 0.41
ErfAct-1	<b>81.41<math>\pm</math>0.45</b>	<b>71.29<math>\pm</math>0.31</b>
ErfAct-2	<b>81.12<math>\pm</math>0.42</b>	<b>71.21<math>\pm</math>0.34</b>

Table 7: Comparison between different baseline activations and ErfAct-1 and ErfAct-2 on semantic segmentation problem on U-NET model in CityScapes dataset. mean $\pm$ std is reported in the table.

Activation Function	BLEU Score on the newstest2014 dataset
ReLU	26.2 $\pm$ 0.15
Swish	26.4 $\pm$ 0.10
Leaky ReLU ( $\alpha = 0.01$ )	26.3 $\pm$ 0.17
ELU	25.1 $\pm$ 0.15
Softplus	23.6 $\pm$ 0.16
Mish	26.3 $\pm$ 0.12
GELU	26.4 $\pm$ 0.19
PReLU	26.2 $\pm$ 0.21
ReLU6	26.1 $\pm$ 0.14
ErfAct-1	<b>26.8<math>\pm</math>0.11</b>
ErfAct-2	<b>26.7<math>\pm</math>0.10</b>

Table 8: Comparison between different baseline activations and ErfAct-1 and ErfAct-2 on Machine translation problem on transformer model in WMT-2014 dataset. mean $\pm$ std is reported in the table.

## 5 Baseline Table

The experiment section shows that ErfAct-1 and ErfAct-2 beat or perform equally well with baseline activation functions in most cases while under-performs marginally on rare occasions. We provide a detailed comparison based on all the experiments in earlier sections and appendix section with the proposed and the baseline activation functions in Table 9.

Baselines	ReLU	Leaky ReLU	ELU	Softplus	Swish	PRELU	ReLU6	Mish	GELU
ErfAct-1 > Baseline	54	54	54	54	51	53	53	50	53
ErfAct-1 = Baseline	0	0	0	0	0	0	0	0	0
ErfAct-1 < Baseline	0	0	0	0	3	1	1	4	1
ErfAct-2 > Baseline	54	54	54	54	51	53	53	50	53
ErfAct-2 = Baseline	0	0	0	0	0	0	0	0	0
ErfAct-2 < Baseline	0	0	0	0	3	1	1	4	1

Table 9: Baseline table for ErfAct-1 and ErfAct-2. These numbers represent the total number of models in which ErfAct-1 and ErfAct-2 underperforms, equal or outperforms compared to the baseline activation functions

## 5.1 Computational Time Comparison

We present the time comparison for the baseline activation functions and ErfAct-1, ErfAct-2 for the mean of 100 runs for both forward and backward pass on a  $32 \times 32$  RGB image in PreActResNet-18 [29] model in Table 10. An NVIDIA Tesla V100 GPU with 32GB ram is used to run the experiments. From Table 10 and the experiment section, it is clear that there is a small trade-off between the computational time and the model performance when compared to ReLU as the proposed activations contain trainable parameters. In contrast, the time is comparable with Swish or Mish and better than GELU and model performance comparatively much better than these three activations in most cases.

Activation Function	Forward Pass	Backward Pass
ReLU	$5.39 \pm 0.39 \mu s$	$5.70 \pm 1.56 \mu s$
Swish	$6.93 \pm 1.12 \mu s$	$9.21 \pm 1.21 \mu s$
Leaky ReLU ( $\alpha = 0.01$ )	$5.50 \pm 0.51 \mu s$	$5.97 \pm 0.75 \mu s$
ELU	$6.17 \pm 0.50 \mu s$	$5.93 \pm 0.93 \mu s$
Softplus	$6.13 \pm 0.49 \mu s$	$5.94 \pm 0.55 \mu s$
Mish	$7.45 \pm 2.55 \mu s$	$8.89 \pm 3.45 \mu s$
GELU	$11.12 \pm 1.52 \mu s$	$10.12 \pm 1.71 \mu s$
PRELU	$6.12 \pm 0.90 \mu s$	$6.23 \pm 1.41 \mu s$
ReLU6	$5.77 \pm 0.73 \mu s$	$5.73 \pm 0.66 \mu s$
ErfAct-1	$7.41 \pm 1.11 \mu s$	$10.51 \pm 1.23 \mu s$
ErfAct-2	$7.53 \pm 1.27 \mu s$	$10.29 \pm 1.58 \mu s$

Table 10: Runtime comparison for the forward and backward passes for ErfAct-1 and ErfAct-2 and baseline activation functions for a  $32 \times 32$  RGB image in PreActResNet-18 model.

## 6 Conclusion

In this work, we propose two simple and effective novel activation functions. We call them ErfAct-1 and ErfAct-2. The method of construction is a combination of functions using trainable parameters. The proposed functions are unbounded above, bounded below, non-monotonic, smooth and zero centred. We show that both functions can approximate the ReLU activation function. Across most of the experiments, ErfAct-1 and ErfAct-2 are top-performing activation functions from which we can conclude that the proposed functions have the potential to replace the widely used activations like ReLU, Swish or Mish.

## References

- [1] Vinod Nair and Geoffrey E. Hinton. Rectified linear units improve restricted boltzmann machines. In Johannes Fürnkranz and Thorsten Joachims, editors, *Proceedings of the 27th International Conference on Machine Learning (ICML-10)*, June 21-24, 2010, Haifa, Israel, pages 807–814. Omnipress, 2010.

- [2] Andrew L. Maas, Awni Y. Hannun, and Andrew Y. Ng. Rectifier nonlinearities improve neural network acoustic models. In *in ICML Workshop on Deep Learning for Audio, Speech and Language Processing*, 2013.
- [3] Djork-Arné Clevert, Thomas Unterthiner, and Sepp Hochreiter. Fast and accurate deep network learning by exponential linear units (elus), 2016.
- [4] Kaiming He, Xiangyu Zhang, Shaoqing Ren, and Jian Sun. Delving deep into rectifiers: Surpassing human-level performance on imagenet classification, 2015.
- [5] Alex Krizhevsky. Convolutional deep belief networks on cifar-10, 2010.
- [6] Alejandro Molina, Patrick Schramowski, and Kristian Kersting. Padé activation units: End-to-end learning of flexible activation functions in deep networks, 2020.
- [7] Koushik Biswas, Shilpak Banerjee, and Ashish Kumar Pandey. Orthogonal-padé activation functions: Trainable activation functions for smooth and faster convergence in deep networks, 2021.
- [8] Ningning Ma, Xiangyu Zhang, Ming Liu, and Jian Sun. Activate or not: Learning customized activation, 2021.
- [9] Diganta Misra. Mish: A self regularized non-monotonic activation function, 2020.
- [10] Dan Hendrycks and Kevin Gimpel. Gaussian error linear units (gelus), 2020.
- [11] Prajit Ramachandran, Barret Zoph, and Quoc V. Le. Searching for activation functions, 2017.
- [12] Koushik Biswas, Sandeep Kumar, Shilpak Banerjee, and Ashish Kumar Pandey. Tanhsoft - dynamic trainable activation functions for faster learning and better performance. *IEEE Access*, pages 1–1, 2021.
- [13] Koushik Biswas, Sandeep Kumar, Shilpak Banerjee, and Ashish Kumar Pandey. Eis - efficient and trainable activation functions for better accuracy and performance. In Igor Farkaš, Paolo Masulli, Sebastian Otte, and Stefan Wermter, editors, *Artificial Neural Networks and Machine Learning – ICANN 2021*, pages 260–272, Cham, 2021. Springer International Publishing.
- [14] Stefan Elfving, Eiji Uchibe, and Kenji Doya. Sigmoid-weighted linear units for neural network function approximation in reinforcement learning, 2017.
- [15] Tsung-Yi Lin, Michael Maire, Serge Belongie, Lubomir Bourdev, Ross Girshick, James Hays, Pietro Perona, Deva Ramanan, C. Lawrence Zitnick, and Piotr Dollár. Microsoft coco: Common objects in context, 2015.
- [16] Alexey Bochkovskiy, Chien-Yao Wang, and Hong-Yuan Mark Liao. Yolov4: Optimal speed and accuracy of object detection, 2020.
- [17] Alec Radford, Jeffrey Wu, Rewon Child, David Luan, Dario Amodei, and Ilya Sutskever. Language Models are Unsupervised Multitask Learners. 2019.
- [18] Tom B. Brown, Benjamin Mann, Nick Ryder, Melanie Subbiah, Jared Kaplan, Prafulla Dhariwal, Arvind Nee-lakantan, Pranav Shyam, Girish Sastry, Amanda Askell, Sandhini Agarwal, Ariel Herbert-Voss, Gretchen Krueger, Tom Henighan, Rewon Child, Aditya Ramesh, Daniel M. Ziegler, Jeffrey Wu, Clemens Winter, Christopher Hesse, Mark Chen, Eric Sigler, Mateusz Litwin, Scott Gray, Benjamin Chess, Jack Clark, Christopher Berner, Sam McCandlish, Alec Radford, Ilya Sutskever, and Dario Amodei. Language models are few-shot learners, 2020.
- [19] Patrick Kidger and Terry Lyons. Universal approximation with deep narrow networks, 2020.
- [20] Y. LeCun, B. Boser, J. S. Denker, D. Henderson, R. E. Howard, W. Hubbard, and L. D. Jackel. Backpropagation applied to handwritten zip code recognition. *Neural Computation*, 1(4):541–551, 1989.
- [21] Yann LeCun, Corinna Cortes, and CJ Burges. Mnist handwritten digit database. *ATT Labs [Online]*. Available: <http://yann.lecun.com/exdb/mnist>, 2, 2010.
- [22] Han Xiao, Kashif Rasul, and Roland Vollgraf. Fashion-mnist: a novel image dataset for benchmarking machine learning algorithms. *arXiv preprint arXiv:1708.07747*, 2017.
- [23] Alex Krizhevsky. Learning multiple layers of features from tiny images. Technical report, University of Toronto, 2009.
- [24] Y. Le and X. Yang. Tiny imagenet visual recognition challenge. 2015.
- [25] Yuval Netzer, Tao Wang, Adam Coates, Alessandro Bissacco, Bo Wu, and Andrew Y Ng. Reading digits in natural images with unsupervised feature learning. 2011.
- [26] Alex Krizhevsky, Ilya Sutskever, and Geoffrey E. Hinton. Imagenet classification with deep convolutional neural networks. In *Proceedings of the 25th International Conference on Neural Information Processing Systems - Volume 1*, NIPS’12, page 1097–1105, Red Hook, NY, USA, 2012. Curran Associates Inc.
- [27] Karen Simonyan and Andrew Zisserman. Very deep convolutional networks for large-scale image recognition, 2015.

- [28] Y. Lecun, L. Bottou, Y. Bengio, and P. Haffner. Gradient-based learning applied to document recognition. *Proceedings of the IEEE*, 86(11):2278–2324, 1998.
- [29] Kaiming He, Xiangyu Zhang, Shaoqing Ren, and Jian Sun. Identity mappings in deep residual networks, 2016.
- [30] Gao Huang, Zhuang Liu, Laurens van der Maaten, and Kilian Q. Weinberger. Densely connected convolutional networks, 2016.
- [31] Mark Sandler, Andrew Howard, Menglong Zhu, Andrey Zhmoginov, and Liang-Chieh Chen. Mobilenetv2: Inverted residuals and linear bottlenecks, 2019.
- [32] Kaiming He, Xiangyu Zhang, Shaoqing Ren, and Jian Sun. Deep residual learning for image recognition, 2015.
- [33] Christian Szegedy, Vincent Vanhoucke, Sergey Ioffe, Jonathon Shlens, and Zbigniew Wojna. Rethinking the inception architecture for computer vision, 2015.
- [34] Sergey Zagoruyko and Nikos Komodakis. Wide residual networks, 2016.
- [35] Forrest N. Iandola, Song Han, Matthew W. Moskewicz, Khalid Ashraf, William J. Dally, and Kurt Keutzer. Squeezenet: Alexnet-level accuracy with 50x fewer parameters and <0.5mb model size, 2016.
- [36] Mingxing Tan and Quoc V. Le. Efficientnet: Rethinking model scaling for convolutional neural networks, 2020.
- [37] Fisher Yu, Dequan Wang, Evan Shelhamer, and Trevor Darrell. Deep layer aggregation, 2019.
- [38] Christian Szegedy, Wei Liu, Yangqing Jia, Pierre Sermanet, Scott Reed, Dragomir Anguelov, Dumitru Erhan, Vincent Vanhoucke, and Andrew Rabinovich. Going deeper with convolutions, 2014.
- [39] Saining Xie, Ross Girshick, Piotr Dollár, Zhuowen Tu, and Kaiming He. Aggregated residual transformations for deep neural networks, 2017.
- [40] François Chollet. Xception: Deep learning with depthwise separable convolutions, 2017.
- [41] Ningning Ma, Xiangyu Zhang, Hai-Tao Zheng, and Jian Sun. Shufflenet v2: Practical guidelines for efficient cnn architecture design, 2018.
- [42] Min Lin, Qiang Chen, and Shuicheng Yan. Network in network, 2014.
- [43] Diederik P. Kingma and Jimmy Ba. Adam: A method for stochastic optimization. In Yoshua Bengio and Yann LeCun, editors, *3rd International Conference on Learning Representations, ICLR 2015, San Diego, CA, USA, May 7-9, 2015, Conference Track Proceedings*, 2015.
- [44] Nitish Srivastava, Geoffrey Hinton, Alex Krizhevsky, Ilya Sutskever, and Ruslan Salakhutdinov. Dropout: A simple way to prevent neural networks from overfitting. *J. Mach. Learn. Res.*, 15(1):1929–1958, January 2014.
- [45] Mark Everingham, Luc Gool, Christopher K. Williams, John Winn, and Andrew Zisserman. The pascal visual object classes (voc) challenge. *Int. J. Comput. Vision*, 88(2):303–338, June 2010.
- [46] Wei Liu, Dragomir Anguelov, Dumitru Erhan, Christian Szegedy, Scott Reed, Cheng-Yang Fu, and Alexander C. Berg. Ssd: Single shot multibox detector. *Lecture Notes in Computer Science*, page 21–37, 2016.
- [47] H. Robbins and S. Monro. A stochastic approximation method. *Annals of Mathematical Statistics*, 22:400–407, 1951.
- [48] J. Kiefer and J. Wolfowitz. Stochastic estimation of the maximum of a regression function. *Annals of Mathematical Statistics*, 23:462–466, 1952.
- [49] Marius Cordts, Mohamed Omran, Sebastian Ramos, Timo Rehfeld, Markus Enzweiler, Rodrigo Benenson, Uwe Franke, Stefan Roth, and Bernt Schiele. The cityscapes dataset for semantic urban scene understanding, 2016.
- [50] Olaf Ronneberger, Philipp Fischer, and Thomas Brox. U-net: Convolutional networks for biomedical image segmentation, 2015.
- [51] Xavier Glorot and Yoshua Bengio. Understanding the difficulty of training deep feedforward neural networks. In Yee Whye Teh and Mike Titterton, editors, *Proceedings of the Thirteenth International Conference on Artificial Intelligence and Statistics*, volume 9 of *Proceedings of Machine Learning Research*, pages 249–256, Chia Laguna Resort, Sardinia, Italy, 13–15 May 2010. JMLR Workshop and Conference Proceedings.
- [52] Ashish Vaswani, Noam Shazeer, Niki Parmar, Jakob Uszkoreit, Llion Jones, Aidan N. Gomez, Lukasz Kaiser, and Illia Polosukhin. Attention is all you need, 2017.
- [53] Sergey Ioffe and Christian Szegedy. Batch normalization: Accelerating deep network training by reducing internal covariate shift, 2015.
- [54] Hao Zheng, Zhanlei Yang, Wenju Liu, Jizhong Liang, and Yanpeng Li. Improving deep neural networks using softplus units. In *2015 International Joint Conference on Neural Networks (IJCNN)*, pages 1–4, 2015.

## A Appendix

In this section, we present more experiments on MNIST, Fashion MNIST, and SVHN datasets with LeNet [28] and an 8-layer homogeneous custom convolutional neural network (CNN) architecture and the results are reported on Table 11 and 13. The custom network is constructed with CNN layers with  $3 \times 3$  kernels and max-pooling layers with  $2 \times 2$  kernels. We have used Channel depths of size 128 (twice), 64 (thrice), 32 (twice), with a dense layer of size 128, Max-pooling layer(thrice), and dropout[44]. We have applied batch-normalization[53] before the activation function layer and more details about this architecture is given in figure 6.

A more detailed experiments on CIFAR10 and CIFAR100 datasets with EfficientNet B0 (EN-B0) [36], LeNet (LN) [28], AlexNet (AN) [26], PreActResnet-18 (PARN-18) [29], Deep Layer Aggregation (DLA) [37], Googlenet (GN) [38], Resnext-50 (Rxt) [39], Xception (Xpt) [40], ShuffleNet V2 (SN-V2) [41], ResNet18 (RN-18) [32], and Network in Network (NIN) [42] is reported in the Table 12 and 14 respectively. We get good improvement with EfficientNet B0, PreActResnet-18, LeNet, GoogleNet, Resnext-50, and ShuffleNet V2 models on both the datasets compared to ReLU or other baseline activation functions.

### A.1 Baseline activation functions

1. **ReLU:** ReLU [1] is one of the most widely used activation function and defined as  $f(x) = \max(x, 0)$ .
2. **Leaky ReLU:** Leaky ReLU [2] is a variant of ReLU in which a linear negative component is added to ReLU. Leaky ReLU is defined as  $f(x) = \max(x, 0.01x)$
3. **Parametric ReLU:** Parametric ReLU (PReLU) [4] is a trainable version of Leaky ReLU. PReLU is defined as  $f(x) = \max(x, \alpha x)$  where  $\alpha$  is the learnable parameter.
4. **ReLU6:** ReLU6 [5] is defined as  $f(x) = \min(\max(x, 0), 6)$ .
5. **ELU:** ELU [3] is defined as  $f(x) = \max(x, 0) + \min(\alpha(e^x - 1), 0)$ .
6. **Softplus:** Softplus [54] is a smoothing of ReLU. SoftPlus is defined as  $f(x) = \ln(1 + e^x)$ .
7. **Swish:** Swish [11] is a trainable activation function found by automated search technique by Google brain team. Swish is defined as  $f(x) = \frac{x}{1 + e^{-\beta x}}$ , where  $\beta$  is a trainable parameter.
8. **GELU:** GELU [10] can be viewed as a smoothing version of ReLU. GELU is defined as  $f(x) = 0.5x(1 + \tanh[\sqrt{\frac{2}{\pi}}(x + 0.044715x^3)])$ .
9. **Mish:** Mish [9] is defined as  $x \tanh(\ln(1 + e^x))$ .

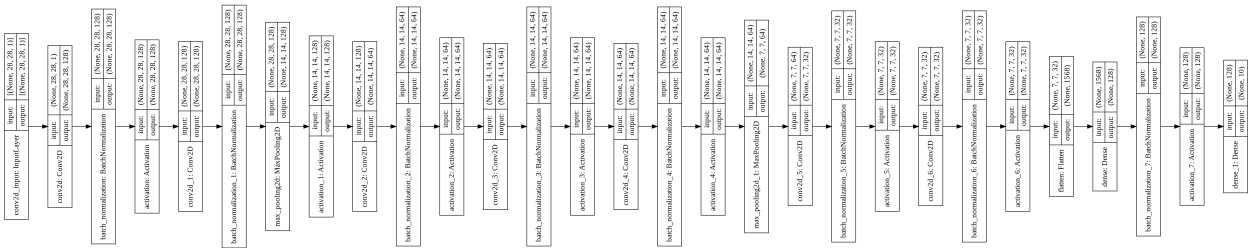


Figure 6: Custom designed network used for evaluation on MNIST, Fashion MNIST, and SVHN

Activation Function	MNIST	Fashion MNIST	SVHN
ReLU	99.09±0.10	92.92±0.21	95.10±0.22
Swish	99.20±0.09	93.04±0.23	95.21±0.23
Leaky ReLU( $\alpha = 0.01$ )	99.14±0.09	92.99±0.22	95.30±0.25
ELU	99.10±0.13	92.91±0.30	95.17±0.27
Softplus	98.95 ±0.17	92.72±0.28	95.08±0.37
Mish	99.32±0.10	93.12±0.21	95.33±0.21
GELU	99.28±0.09	93.19±0.22	95.22±0.24
PReLU	99.08±0.17	92.89±0.35	95.15±0.30
ReLU6	99.17±0.12	92.99±0.20	95.17±0.22
ErfAct-1	<b>99.42±0.08</b>	<b>93.42±0.23</b>	<b>95.49±0.24</b>
ErfAct-2	<b>99.40±0.08</b>	<b>93.35±0.20</b>	<b>95.55±0.23</b>

Table 11: Comparison between different baseline activations and ErfAct-1 and ErfAct-2 on MNIST, Fashion MNIST, and SVHN datasets with Custom designed network. 10-fold mean accuracy (in %) have been reported. mean±std is reported in the table.

Activation Function	EN-B0	LN	AN	PARN-18	DLA	GN	Rxt	Xpt	SN-V2	RN-18	NIN
ReLU	91.05 ±0.27	67.24 ±0.34	89.25 ±0.37	90.41 ±0.32	89.30 ±0.34	91.18 ±0.35	91.60 ±0.39	90.12 ±0.38	90.10 ±0.32	90.26 ±0.40	87.12 ±0.38
Leaky ReLU ( $\alpha = 0.01$ )	91.19 ±0.29	67.12 ±0.37	89.49 ±0.28	90.61 ±0.31	89.24 ±0.37	91.42 ±0.33	91.51 ±0.34	90.20 ±0.39	90.12 ±0.31	90.30 ±0.36	87.01 ±0.39
ELU	91.15 ±0.25	67.11 ±0.40	89.38 ±0.40	90.77 ±.35	89.47 ±0.34	91.59 ±0.38	91.48 ±0.31	90.22 ±0.42	90.25 ±0.36	90.42 ±0.39	87.21 ±0.34
Swish	91.64 ±0.24	67.95 ±0.35	89.42 ±0.27	90.84 ±0.30	89.45 ±0.32	91.89 ±0.35	91.75 ±0.34	90.54 ±0.40	90.63 ±0.30	90.99 ±0.36	87.89 ±0.35
Softplus	90.54 ±0.34	67.01 ±0.42	89.07 ±0.38	90.20 ±0.39	89.05 ±0.39	91.19 ±0.37	91.30 ±0.45	89.66 ±0.42	89.99 ±0.39	90.01 ±0.41	86.65 ±0.42
Mish	91.89 ±0.24	68.25 ±0.35	89.67 ±0.26	91.35 ±0.30	89.64 ±0.29	92.23 ±0.39	92.15 ±0.32	<b>90.64</b> ±0.41	90.94 ±0.35	91.06 ±0.33	<b>87.95</b> ±0.39
GELU	91.65 ±0.22	67.66 ±0.39	89.22 ±0.28	90.99 ±0.32	89.69 ±0.34	91.60 ±0.32	92.05 ±0.39	90.59 ±0.43	90.89 ±0.35	90.87 ±0.31	87.45 ±0.39
PReLU	90.88 ±0.29	67.38 ±0.39	89.45 ±0.40	90.49 ±0.32	89.39 ±0.37	91.39 ±0.34	91.59 ±0.42	90.53 ±0.40	90.19 ±0.36	90.29 ±0.31	87.32 ±0.37
ReLU6	91.25 ±0.25	67.39 ±0.36	89.22 ±0.35	90.59 ±0.33	89.22 ±0.35	91.29 ±0.32	91.89 ±0.35	90.51 ±0.38	90.19 ±0.31	90.39 ±0.45	87.44 ±0.36
ErfAct-1	<b>92.96</b> ±0.22	<b>69.23</b> ±0.36	<b>90.59</b> ±0.22	<b>91.95</b> ±0.31	<b>90.39</b> ±0.31	<b>93.33</b> ±0.37	<b>93.29</b> ±0.29	90.42 ±0.41	<b>91.41</b> ±0.31	<b>92.36</b> ±0.28	87.75 ±0.35
ErfAct-2	<b>92.89</b> ±0.23	<b>69.12</b> ±0.36	<b>90.78</b> ±0.20	<b>91.89</b> ±0.32	<b>90.56</b> ±0.31	<b>93.21</b> ±0.35	<b>93.10</b> ±0.28	90.50 ±0.40	<b>91.49</b> ±0.29	<b>92.30</b> ±0.29	87.79 ±0.33

Table 12: Comparison between different baseline activations and ErfAct-1 and ErfAct-2 on CIFAR10 dataset. Top-1 accuracy(in %) for mean of 12 different runs have been reported. mean±std is reported in the table.

Activation Function	MNIST	Fashion MNIST	SVHN
ReLU	98.95±0.11	91.00±0.20	93.17±0.24
Swish	99.04±0.11	91.15±0.22	93.22±0.21
Leaky ReLU( $\alpha = 0.01$ )	99.02±0.10	91.05±0.20	93.25±0.24
ELU	98.95±0.12	91.98±0.28	93.11±0.24
Softplus	98.81 ±0.14	90.81±0.29	93.08±0.37
Mish	99.12±0.11	91.12±0.21	93.30±0.21
GELU	99.15±0.10	91.17±0.20	93.22±0.21
PReLU	99.01±0.17	90.89±0.25	93.05±0.28
ReLU6	99.7±0.10	90.99±0.24	93.10±0.20
ErfAct-1	<b>99.30±0.08</b>	<b>91.37±0.20</b>	<b>93.52±0.21</b>
ErfAct-2	<b>99.32±0.08</b>	<b>91.31±0.22</b>	<b>93.43±0.21</b>

Table 13: Comparison between different baseline activations and ErfAct-1 and ErfAct-2 on MNIST, Fashion MNIST, and SVHN datasets with LeNet model. 10-fold mean accuracy (in %) have been reported. mean±std is reported in the table.

Activation Function	EN-B0	LN	AN	PARN-18	DLA	GN	Rxt	Xpt	SN-V2	RN-18	NIN
ReLU	67.20 ±0.47	32.35 ±0.60	59.89 ±0.56	61.19 ±0.49	63.19 ±0.51	70.32 ±0.39	69.89 ±0.42	63.57 ±0.45	64.15 ±0.47	61.15 ±0.51	60.24 ±0.53
Leaky ReLU ( $\alpha = 0.01$ )	67.39 ±0.50	32.19 ±0.67	60.15 ±0.52	61.20 ±0.45	63.52 ±0.52	70.10 ±0.45	69.75 ±0.40	63.42 ±0.49	64.31 ±0.41	61.22 ±0.50	60.19 ±0.49
ELU	67.12 ±0.54	32.25 ±0.62	60.38 ±0.53	61.35 ±0.51	63.54 ±0.55	70.43 ±0.49	69.65 ±0.45	63.45 ±0.43	64.56 ±0.46	61.23 ±0.50	60.12 ±0.54
Swish	67.75 ±0.42	34.46 ±0.61	60.23 ±0.55	63.72 ±0.44	63.42 ±0.52	70.52 ±0.40	70.29 ±0.38	64.09 ±0.41	64.90 ±0.45	61.65 ±0.48	<b>60.89</b> ±0.50
Softplus	67.01 ±0.55	32.12 ±0.63	59.46 ±0.61	60.78 ±0.56	63.10 ±0.55	70.01 ±0.51	69.97 ±0.45	63.23 ±0.47	64.12 ±0.51	61.15 ±0.49	60.12 ±0.55
Mish	68.06 ±0.41	34.49 ±0.58	60.89 ±0.58	63.89 ±0.47	63.56 ±0.50	70.83 ±0.41	70.89 ±0.39	<b>64.42</b> ±0.40	65.09 ±0.44	62.01 ±0.48	60.65 ±0.49
GELU	67.64 ±0.42	67.66 ±0.64	60.44 ±0.52	63.12 ±0.48	63.32 ±0.56	70.78 ±0.40	70.65 ±0.39	64.01 ±0.46	64.67 ±0.42	61.42 ±0.49	60.42 ±0.52
PReLU	67.01 ±0.51	32.12 ±0.64	59.99 ±0.62	61.28 ±0.55	63.42 ±0.50	70.41 ±0.36	69.71 ±0.47	63.59 ±0.49	64.23 ±0.46	61.43 ±0.53	60.13 ±0.59
ReLU6	67.35 ±0.47	32.26 ±0.58	59.56 ±0.57	61.22 ±0.52	63.42 ±0.45	70.52 ±0.38	69.72 ±0.46	63.51 ±0.46	64.12 ±0.45	61.32 ±0.46	60.37 ±0.49
ErfAct-1	<b>69.05</b> ±0.39	<b>35.52</b> ±0.56	<b>61.89</b> ±0.59	<b>65.65</b> ±0.50	<b>64.56</b> ±0.47	<b>72.30</b> ±0.43	<b>71.89</b> ±0.44	64.21 ±0.41	<b>66.49</b> ±0.41	<b>63.32</b> ±0.50	60.60 ±0.45
ErfAct-2	<b>68.92</b> ±0.41	<b>35.67</b> ±0.51	<b>61.57</b> ±0.55	<b>65.32</b> ±0.52	<b>64.65</b> ±0.51	<b>72.12</b> ±0.45	<b>71.75</b> ±0.48	64.15 ±0.40	<b>66.45</b> ±0.49	<b>63.45</b> ±0.41	60.56 ±0.47

Table 14: Comparison between different baseline activations and ErfAct-1 and ErfAct-2 on CIFAR100 dataset. Top-1 accuracy(in %) for mean of 12 different runs have been reported. mean±std is reported in the table.